Intracerebral Expression of AAV-APOE4 Is Not Sufficient to Alter Tau Burden in Two Distinct Models of Tauopathy

Emily J. Koller [1,2] · Elsa Gonzalez De La Cruz [2] · Mary Weinrich [2] · Tosha Williams [1,2] · Pedro E. Cruz [2] · Daniel Ryu [2] · Todd E. Golde [1,2,3] · Patrick M. Sullivan [4] · Jada Lewis [1,2,3] · David R. Borchelt [1,2,3] · Paramita Chakrabarty [1,2,3] ●

Abstract

Apolipoprotein E4 (*APOE4*) is the major genetic risk factor for sporadic Alzheimer's disease (AD), which is characterized by amyloid β (Aβ) plaques and tau tangles. Though the role of APOE4 in Aβ pathogenesis has been mechanistically defined in rodent models, much less is known regarding the relationship of APOE4 to tau pathogenesis. Recent studies have indicated a possible correlation between APOE isoform-dependent alterations in tau pathology and neurodegeneration. To explore whether neuronal expression of APOE4 triggers tauopathy, here we delivered adeno-associated viruses (AAV) expressing human APOE4 in two different models of tauopathy—rTg4510 and PS19 lines. Intracerebroventricular delivery of AAV-APOE4 in neonatal rTg4510 and PS19 mice resulted in increased APOE4 protein in neurons but did not result in altered phosphorylated tau burden, pretangle tau pathology, or silver-positive tangle pathology. Biochemical analysis of synaptic proteins did not reveal substantial alterations. Our results indicate that over-expression of APOE4 in neurons, using an AAV-mediated approach, is not sufficient to accelerate or otherwise alter the inherent tau pathology that occurs in mice overexpressing mutant human tau.

Keywords Phosphorylated tau · Apolipoprotein E4 · rTg4510 · PS19 · Neurofibrillary tangle

Abbreviations

AAV	adeno-associated viruses
Aβ	amyloid β
APOE	human apolipoprotein E
Apoe	mouse apolipoprotein E
APOE4 TR	APOE E4 allele-targeted replacement
AD	Alzheimer's disease
CaMKII	Ca^{2+}/calmodulin-dependent protein kinase II
CBA	cytomegalovirus enhancer/chicken β-actin
EGFP	enhanced green fluorescent protein
GFAP	glial fibrillary acidic protein
Iba-1	ionized calcium binding adaptor molecule 1
MAPT	microtubule-associated protein tau
NFT	neurofibrillary tangle
PSP	progressive supranuclear palsy
ptau	phosphorylated tau
Tg	transgenic

✉ Paramita Chakrabarty
pchakrabarty@ufl.edu

1 Department of Neuroscience, University of Florida, Gainesville, FL 32610, USA

2 Center for Translational Research in Neurodegenerative Disease, University of Florida, Gainesville, FL 32610, USA

3 McKnight Brain Institute, University of Florida, Gainesville, FL 32610, USA

4 Department of Medicine, Duke University, Durham VA Geriatric Research, Education and Clinical Center, Durham, NC 27710, USA

Introduction

Human apolipoprotein E (*APOE*) exists as three allelic variants—E2, E3, and E4, with the E4 variant significantly increasing the risk of developing Alzheimer's disease (AD). Indeed, *APOE4* homozygotes are at 12× higher susceptibility to develop AD, making it the most significant risk gene for sporadic AD [1]. APOE functions as a lipoprotein and is critical for maintaining lipid homeostasis in the periphery and brain [2]. It is thought that the E4 variant confers toxic gain of function(s) leading to impaired clearance of protein aggregates, decreased brain activity, altered synaptic plasticity, and loss of neuroprotective functions [3].

Several epidemiologic and imaging studies have confirmed a direct pathologic correlation between APOE4 isoform and amyloid β (Aβ) burden in AD patients [4]. Rodent studies have confirmed that APOE4 plays a critical role in Aβ production, aggregation, and clearance, clearly indicating a mechanistic link between APOE4 and AD-type amyloid pathology [5–10]. Whether APOE4 has a similar pathogenic role in modulating tau, another canonical neuropathological hallmark of AD, remains contentious. In patients, APOE4 has been associated with neurofibrillary tangles (NFTs), but only if these patients have substantial Aβ pathology [11]. Further, another recent study reported that female APOE4+ AD patients have higher tau levels in their CSF, only if these patients have substantial Aβ pathology [12]. Interestingly, APOE2, considered the protective allele for AD, has been identified as a risk factor for the tauopathy disorder, progressive supranuclear palsy (PSP) [13]. Taken together, there is a general lack of consensus regarding the effects of APOE isoform(s) on human tauopathy.

The first definitive report of an association between APOE and tau in a preclinical model showed that the PS19 mouse model of tauopathy had significant neurodegeneration and altered tau burden in the presence of the APOE4 allele but not APOE3 or APOE2 alleles [14]. A subsequent report, however, uncovered a pathogenic link between APOE2 and tauopathy in rodent models, and with no observed effect of APOE4 on tau pathology [13]. In light of such disparate observations, we sought to test the hypothesis that intracerebral expression of APOE4 will lead to exacerbated tau pathologies and reduced synaptic integrity in mouse models of tauopathy. We used recombinant adeno-associated viruses (AAV) to express human APOE4 in the CNS following intracerebral delivery of AAV into neonatal rTg4510 or PS19 mouse models that overexpress human 4R tau. In these mice,, we observed that expression of APOE4 did not significantly alter levels of soluble phosphorylated tau (ptau) or conformationally altered tau. Our data suggest that neuronal APOE4 expression, by itself, is not sufficient to induce tau pathogenesis in rodent models of tauopathy.

Materials and Methods

Mice

rTg4510, PS19, and APOE4-targeted replacement (APOE4-TR) mice were maintained in house. Parent rTg4510 mice were obtained from Dr. J. Lewis (University of Florida), PS19 mice were obtained from Jackson Labs (Stock No: 024841), and APOE4-TR mice were obtained from Dr. P. Sullivan (Duke University). The rTg4510 mice were generated by crossing the 4510 responder line expressing human P301L mutant microtubule-associated protein tau (MAPT) with the CaMKIIα-tTA activator line [15]. PS19 mice express

the P301S mutant MAPT driven by the mouse prion protein promoter and maintained on B6/C3H background [16]. The APOE4-TR mice were originally created by homologous recombination to replace the endogenous mouse apoE coding exons with human APOE4 exons [17]. Mice lived under a 12-h light/dark cycle, were group housed, and had free access to food and water. Pre-approval was obtained from Institutional Animal Care and Use Committee in accordance with University of Florida policies for all mouse husbandry and experimental procedures.

Two separate cohorts of rTg4510 mice were set up and aged to either 4 months or 6 months and one cohort of PS19 mice was set up and aged to 3 months (Table 1). Mice were euthanized and their brains were harvested and cut into sagittal halves. One half was flash frozen and stored at −80 °C while the other half was fixed in 10% normal buffered formalin.

AAV injections

Recombinant adeno-associated viruses serotype 1 (rAAV1) were prepared as previously described [18]. Neonatal rTg4510 or PS19 mice received bilateral intracerebral ventricular injections of rAAV1 (2×10^{11} vector genomes) expressing human APOE4 under the control of the cytomegalovirus enhancer/chicken β-actin (CBA) promoter. The control groups were comprised of either naïve, AAV-enhanced green fluorescent protein (EGFP) injected, or empty capsid (CTR0) injected rTg4510 or PS19 mice. APOE/NeuN-immunopositive cells were counted manually to determine extent of APOE in neurons. APOE/GFAP-immunopositive cells were counted manually to determine the extent of APOE in astrocytes. For each group, one slide was stained per mouse ($n = 3$), and three fields of view in the cortex and hippocampus were quantified (20× field of view, Keyence BZ-X710 All-in-one Fluorescence Microscope) by a blinded observer. Cell counts were averaged within mice.

Immunohistochemical analysis

Following fixation, sagittal hemibrains were dehydrated, embedded in paraffin, and sectioned at 5 μm thickness. Immunohistochemical analysis of brain sections was conducted with a panel of primary antibodies (Table 2) using protocols described earlier [19]. For co-immunofluorescence staining, sections were incubated with Alexa Fluor conjugated secondary antibodies (Invitrogen) and mounted using 4′, 6-diamidino-2-phenylindole (DAPI) containing mounting media (Southern Biotech).

Histological staining

Gallyas silver impregnation protocol was modified from [20]. Briefly, sections were rehydrated and incubated for 5 min in 5% periodic acid. Following two 5 min washes in water,

Table 1 Cohort sizes used in the study

rTg4510		No AAV	AAV-EGFP	Empty capsid(AAV-CTR0)	AAV-APOE4
4 month	M	–	2	1	3
	F	5	1	3	4
Total		12			7
6 month	M	7	–	0	3
	F	3	–	2	2
Total		12			5
PS19		No AAV	AAV-EGFP	Empty capsid(AAV-CTR0)	AAV-APOE4
3 month	M	4	2	–	7
	F	1	2	–	4
Total		9			11

Table 2 List of antibodies used

Primary antibody	Dilution	Retrieval	Secondary antibody	Source	Catalog #
Immunohistochemistry					
CP13	1:4500	Water	Mouse	Peter Davies	N/A
GFAP	1:2000	Water	Rabbit	Dako	Z0334
SQSTM1 (p62)	1:1000	Water	Rabbit	Proteintech	18420–1-AP
Alz50	1:1000	Water	Mouse	Peter Davies	N/A
MC1	1:4000	Water	Mouse	Peter Davies	N/A
AT8	1:10,000	Water	Mouse	ThermoScientific	MN1020
Iba-1	1:1000	Citrate	Rabbit	Wako	019–19741
Co-immunoflourescence					
APOE	1:1000	Water	Rabbit	Abcam	ab24139
NeuN	1:100	Water	Mouse	Millipore	MAB377
GFAP-Cy3	1:1500	Water	–	Sigma	C9205
Donkey anti-mouse IgG (H + L) secondary antibody, Alexa Fluor 594 conjugate	1:1000	–	–	Life Technologies	A21203
Chicken anti-rabbit IgG (H + L) secondary antibody, Alexa Fluor 488 conjugate	1:1000	–	–	Life Technologies	A21441
Western blotting					
APOE	1:500	–	Goat	Millipore	AB947
CP27	1:500	–	Mouse	Peter Davies	N/A
GFAP	1:1000	–	Rabbit	Dako	Z0334
CP13	1:500	–	Mouse	Peter Davies	N/A
PHF1	1:500	–	Mouse	Peter Davies	N/A
T49	1:500	–	Mouse	Millipore	MABN827
GAPDH	1:1000	–	Rabbit	Abcam	ab181602
β actin (AC-15)	1:1000	–	Mouse	Sigma	A5441
Synaptogyrin 3 (E-11)	1:500	–	Mouse	Santa Cruz	sc271046
Synaptophysin	1:500	–	Rabbit	ThermoFisher	PA11043
Spinophilin (EIE7R)	1:500	–	Rabbit	Cell Signaling	14136P
PSD95 (D27E11)	1:500	–	Rabbit	Cell Signaling	3450P
vGlut1	1:1000	–	Mouse	Millipore	MAB5502
GluR1	1:1000	–	Rabbit	Millipore	ABN241

sections were incubated in alkaline silver iodide solution for 1 min and then washed in 0.5% acetic acid for 10 min. Next, slides were placed in developer solution (prepared immediately before use) for 4–6 min. Following development, slides were washed in 0.5% acetic acid for 3 min and then water for 5 min. This was followed by: 5 min incubation in 0.1% gold chloride, rinsing in dH_2O, 5 min incubation in 1% sodium thiosulphate solution, and rinsing in tap water. Sections were then dehydrated, cleared, and mounted. Hematoxylin and eosin (H&E) staining was conducted according to standard histochemical procedures. Briefly, sections were rehydrated and placed in hematoxylin (Sigma, MO) for 5 min and then rinsed in tap water. Next, slides were incubated for 30 sec in 70% ethanol and then dipped four times in 5% eosin (Sigma) followed by clearing in 70% ethanol. Sections were then dehydrated and mounted.

Image analysis

Immunostained and histological images were captured using a Scanscope XT image scanner (Aperio, Vista, CA, USA). Percent immunoreactivity was computed using the Aperio Positive Pixel Count program (Aperio, Vista, CA, USA). One section per brain was quantified for each stain, and the brain regions (cortex and hippocampus) to be quantified were defined by the Paxinos and Franklin's atlas (Mouse Brain in Stereotaxic Coordinates brain atlas). The data is presented as the average % immunoreactivity ± S.E.M. per group. Statistical comparisons were conducted using unpaired t tests or two-way ANOVA with a Sidak post hoc test, if necessary (GraphPad Prism 7). Fluorescent images were captured using an Olympus BX51 fluorescence microscope mounted with a DP71 digital camera (Olympus, Center Valley, PA).

## Hippocampal cell count and cortical thickness analysis

Scanscope XT scanner was used to capture images of stained H&E slides (Aperio, Vista, CA, USA). Brain sections were aligned at approximately 0.96 mm lateral from Bregma using coordinates from Paxinos and Franklin's Mouse Brain in Stereotaxic Coordinates. Regions of the hippocampus (CA1, CA2, and CA3) were defined using the same brain atlas. Three sections between 0.84 and 1.08 mm lateral from Bregma were chosen per brain, and a blinded experimenter counted the number of nuclei in the CA1–CA3 and summed them for each brain. Data are presented as the average cell count in CA1–CA3 for each experimental group ± S.E.M. Statistical comparisons were conducted using an unpaired t-test. Cortex thickness analysis was conducted in the same way. Three sections between 0.84 and 1.08 mm lateral from Bregma were chosen per brain, and a blinded experimenter drew three lines perpendicular from the corpus callosum to the

Fig. 1 AAV-APOE4 transduction in neonatal rTg4510 mice results in robust upregulation of brain APOE4. Neonatal rTg4510 mice were injected with AAV-APOE4 and aged to 4 months (**a**, **b**) or 6 months old (**c**, **d**). Quantification of APOE protein band normalized to actin loading control shows upregulation of APOE4 protein (**b**, **d**). $n = 4$–6 mice/group. Unpaired t-test. $*p < 0.05$; $**p < 0.01$. Representative co-immunofluorescence images showing APOE colocalizing with GFAP or NeuN antibodies on AAV-APOE4 expressing 4-month-old rTg4510 brain sections shows APOE expression from GFAP-immunopositive astrocytes (**e**) and NeuN-immunopositive neurons (**f**). Brains from naïve rTg4510 (top and middle panels) and APOE4 TR mice (bottom panel) are shown (**e**, **f**). Arrows, astrocyte (**e**) or neuron (**f**); arrowhead, vasculature (**e**, **f**). Scale Bar, Merge: 50 μm; 10 μm (zoomed inset in Merge panel). Western blot showing CP27-immunoreactive total human tau levels in 4- (**g**, **h**) and 6-month-old (**i**, **j**) rTg4510 mice. Quantification of tau protein band normalized to GAPDH loading control shows no changes in transgenic tau expression (**h**, **j**). $n = 4$–6/group. Unpaired t test. Black symbols, male mice; gray symbols, female mice.

outer edge of the frontal, motor/sensory, and auditory cortices. The lengths of these lines were averaged per brain. Data are presented as the average cortex thickness for each part of the cortex for each experimental group ± S.E.M. Statistical comparisons were conducted using two-way ANOVA with a Sidak post hoc test, if necessary (GraphPad Prism 7).

Biochemical fractionation of brains

Fractionation protocol was modified from [19]. The appropriate amount of TBS buffer (50 mM Tris base, 274 mM NaCl, 5 mM KCl, pH 8.0) containing protease and phosphatase inhibitors (Pierce Protease & Phosphatase Inhibitor Mini Tablets, ThermoScientific) was added to each frozen brain to achieve a final concentration of 150 mg/mL. Brain homogenization was completed using Tissue Master hand held homogenizer (Omni International). Brain homogenates were centrifuged (Optima MaxE) for 30 min at 22 k rpm at 4 °C. Supernatant (S1) was removed, aliquoted, and stored at −80 °C. The remaining pellet (P1) was resuspended by vortexing in high salt buffer plus 0.5% Triton X-100 (Fisher; 10 mM Tris, 0.8 M NaCl, 10% Sucrose, 0.5% Triton X-100) containing 1X protease and phosphatase inhibitors (Pierce Protease & Phosphatase Inhibitor Mini Tablets, ThermoScientific), and centrifuged for 30 min at 22 k rpm at 4 °C. The resulting supernatant (S2) was removed, aliquoted, and stored at −80 °C. The pellet (P2) was resuspended by vortexing in high salt buffer containing 1% sarkosyl solution. Then samples were incubated for 1 h at 37 °C with gentle shaking, followed by centrifugation at 60 k rpm at 15 °C for 1 h. Once again, the supernatant was removed (S3), aliquoted, and stored at −80 °C. The residual pellet was resuspended in 4M urea/2%SDS by sonicating briefly (Misonix sonicator). A final centrifuging step for 1 h at 50 k rpm at 20 °C resulted in a final supernatant (S4), which was aliquoted, and a pellet (P4).
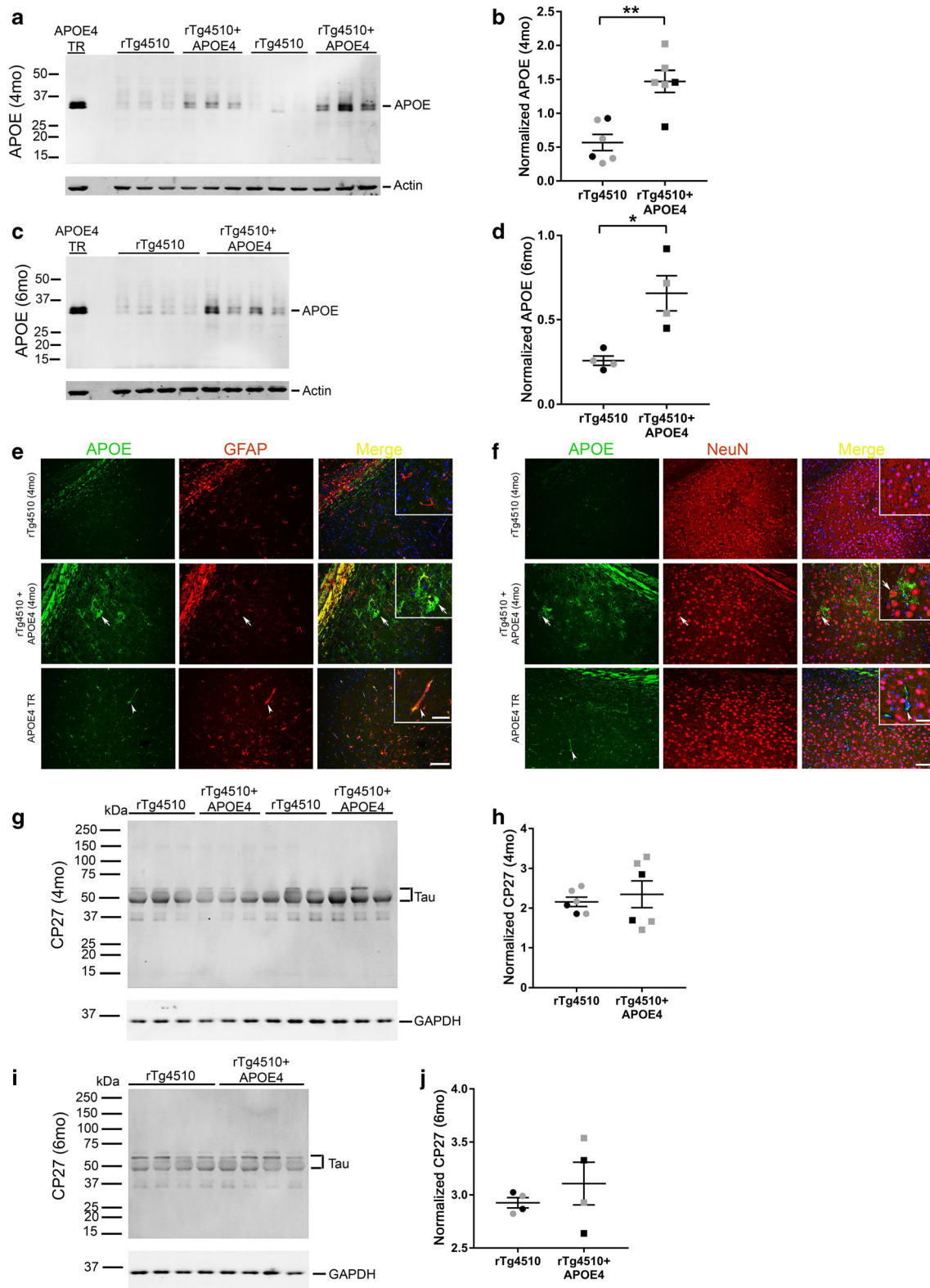
Western blots

Bicinchoninic acid assay (Pierce BCA Protein Assay Kit, ThermoScientific) was used to determine protein concentrations of S1 and S4 brain fractions. Fifteen to 30 μg of total protein from the S1 fraction were loaded per sample per well in a 4–20% Tris-glycine gel (Novex, Invitrogen). Approximately 1 μg of total protein was loaded per sample
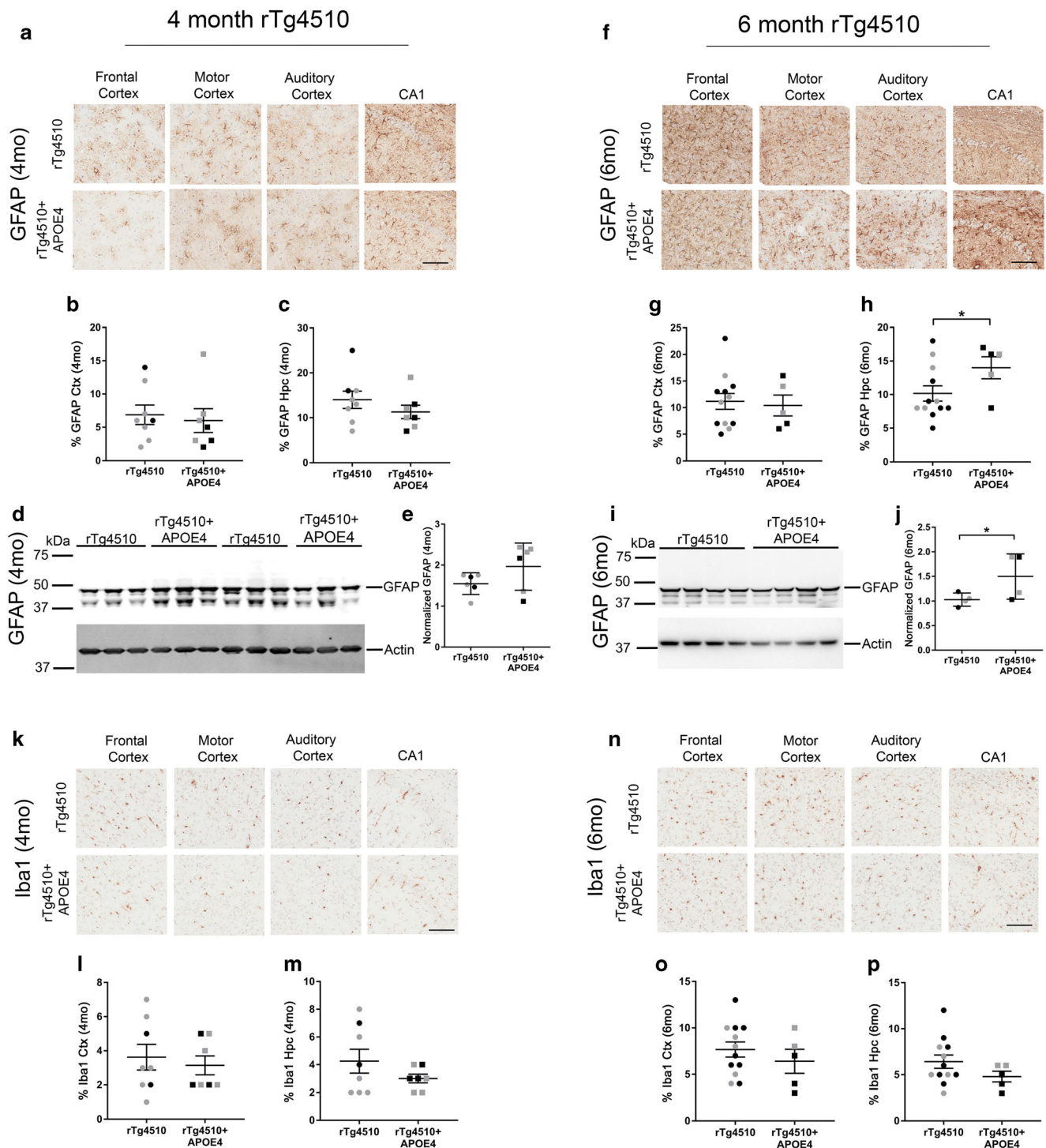
Fig. 2 Analysis of gliosis in rTg4510 mice expressing human APOE4. Neonatal rTg4510 mice injected with AAV-APOE4 and aged to 4 months (a–e, k–m) or 6 months old (f–j, n–p). Anti GFAP antibody was used to examine astrocytosis (a–j) while Iba-1 antibody was used to examine microgliosis (k–p). Representative images of GFAP immunoreactivity and Iba-1 immunoreactivity are shown from different regions of the cortex and hippocampal CA1 (a, f, k, n). Scale bar: 100 μm. Quantitation of the GFAP immunostaining is presented as % immunoreactivity in the cortex (Ctx) or hippocampus (Hpc) (b, c, g, h). $n = 5–12$ mice/group. Unpaired t test. $*p < 0.05$. Following western blotting with GFAP antibody (d, i), bands were standardized to Actin, a housekeeping gene, and quantitated (e, j). $n = 4–6$ mice/group. Unpaired t test. $*p < 0.05$. Quantitation of the Iba-1 immunostaining is presented as % immunoreactivity in the cortex (Ctx) or hippocampus (Hpc) (l, m, o, p). $n = 5–12$ mice/group. Unpaired t test. $*p < 0.05$. Black symbols, male mice; gray symbols, female mice.

per well for the S4 fraction. Electrophoresis was run for 1–1.5 h at 120 V using a Mini Gel Tank (Invitrogen). Protein was transferred to Immobilon-PSQ transfer membranes at 15 V for 40 min using Trans-Blot SD Semi-Dry Transfer Cell (Bio-Rad). Next, membranes were blocked for 1 h in 0.5% casein and then incubated in the appropriately diluted primary antibody (Table 2) overnight at 4 °C. The following day, membranes were washed three times (5 min each) in 1X TBS. Then membranes were incubated at room temperature in the appropriate secondary antibody (Table 2) diluted in 0.5% casein (1:20,000) with 0.005% SDS for 1 h. Following three more washes of the membranes in in 1X TBS for 5 min, protein bands were detected using the multiplex Li-Cor Odyssey Infrared Imaging system (Li-Cor Biosciences, Lincoln, NE, USA). Relative band intensity was quantified using ImageJ software (NIH). Data are presented as average relative band intensity (normalized to loading control) ± S.E.M. Statistical comparisons were performed using unpaired t tests (GraphPad Prism 7).

Results

Increased APOE4 expression in AAV-APOE4-transduced rTg4510 mice

We utilized neonatal delivery of recombinant AAV to establish a somatic model of APOE4 expression in the rTg4510 mouse model of tauopathy. We have demonstrated previously that intracerebral injection of recombinant AAV in neonatal mice leads to widespread gene expression from the CNS [18]. Here, we expressed human APOE4, CTR0 (empty AAV vector) or EGFP in the rTg4510 mouse model of tauopathy by injecting recombinant AAV capsid 1 in neonatal mouse brains (Fig. 1). The rTg4510 model expresses CaMKII-driven P301L tau under the control of the tetracycline activator such that tau expression is suppressed in the presence of doxycycline [21]. We used MAPT$^+$/tTA$^+$ mice that were maintained on normal diet for all the data analyses which will be referred to as transgenic (Tg) mice henceforth. These Tg mice were aged to 4 months with the hypothesis that if neuronal APOE4 were to trigger tauopathy, an earlier timepoint will be sufficient to reveal the pathologic effects. We also incorporated an additional 6-month timepoint to examine APOE effects at ages when robust tau pathology is observed with neurodegeneration [21]. Immunoblotting showed that AAV-driven APOE4 in 4-month-old Tg and 6-month-old Tg mice resulted in increased APOE4 protein levels compared to age-matched control Tg mice (2.58× and 2.53× higher than endogenous mouse Apoe respectively, $p < 0.05$; Fig. 1a–d). We also included brains from APOE4-TR mice to provide a comparison to our AAV model [13, 14, 17]. We observed that the levels of APOE4 were higher in the brains of these APOE4-TR mice

compared to AAV-APOE4 mice (3.2×, Suppl. Fig. 1A-B). Immunofluorescence analysis indicated that AAV-APOE4 was expressed from both astrocytes and neurons in 4-month-old Tg mice (Fig. 1e, f, Suppl. Fig. 1C–F). In the APOE4-TR mice, however, we detected APOE4 primarily in astrocytes and endothelial cells, with no expression in neurons (Fig. 1e, f, arrowhead, Suppl. Fig. 1C-F). We next confirmed that transduction with AAV-APOE4 did not alter the expression of the human *MAPT* transgene in either 4- or 6-month-old Tg mice (Fig. 1g–j). Neuronal expression of APOE4 seemed to modestly increase astrogliosis, as evidenced by immunohistochemical and immunoblotting analysis using GFAP, an astrocyte-specific marker (Fig. 2a–j). In 4-month-old Tg mice expressing AAV-APOE4, GFAP immunoreactivity was unchanged in both cortex and hippocampus compared to age-matched Tg control mice (Fig. 2a–c). This was further confirmed by GFAP immunoblotting (Fig. 2d, e). In 6-month-old Tg mice, we observed increased GFAP in the hippocampus but not in the cortex of AAV-APOE4-expressing mice compared to control mice (Fig. 2f–h, $p < 0.05$). Immunoblotting also confirmed modestly increased GFAP levels in this older group of AAV-APOE4-expressing Tg mice (Fig. 2i, j; $p < 0.05$). Next, we used anti Iba-1 antibody to examine microglial activation in these mice (Fig. 2k–p). In 4- and 6-month-old Tg mice, Iba-1 immunoreactivity remained unchanged between the AAV-APOE4 and control cohorts (Fig. 2k–p).

APOE4 expression does not induce phosphorylated tau or conformationally altered tau in rTg4510 mice

We next examined levels of phosphorylated tau (ptau) and conformationally altered tau in AAV-APOE4-expressing 4- and 6-month-old Tg mice compared to controls. We used two antibodies that recognize ptau epitopes: CP13 (pSer202) and AT8 (pSer202/Thr205) (Fig. 3; Suppl. Fig. 2). CP13 immunoreactivity analysis in 4-month-old mice (Fig. 3a–c) or 6-month-old mice (Fig. 3j–l) showed no appreciable difference across different regions of the brain. Since we observed noticeable APOE expression within neurons in the AAV-APOE4-injected Tg group, we wanted to examine whether individual neurons with high amounts of APOE4 showed higher levels of ptau. We did not observe a direct correlation between the presence of intraneuronal APOE4 with induction of ptau immunoreactivity within the cell, suggesting that high amounts of neuronal APOE4 do not necessarily trigger tauopathy in individual cells (Suppl. Fig. 1G). Further, immunoblotting of the TBS-soluble Tg brain lysates also failed to show any alterations in ptau between AAV-APOE4-expressing mice and controls at either age (Fig. 3d–g, m–p). These data are supported by similar observations from AT8 immunoreactivity in these mice (Suppl. Fig. 2A-F). Interestingly, though unchanged at 4 months of age (Fig.

3h, i), endogenous mouse tau levels were increased in APOE4-expressing Tg mice compared to control mice at 6 months of age (Fig. 3q,r , $p < 0.05$).

Given that Tg mice show robust tangle pathology even at 4 months of age, we next examined whether APOE4 altered pretangle pathology or AD-type NFT pathology in Tg mice (Fig. 4, Suppl. Fig. 3). Initial examination of pretangle pathology using the conformational tau antibodies, MC1 and Alz 50 revealed that MC1-immunopositive tau pathology in the hippocampus was reduced in 4-month-old AAV-APOE4-expressing mice (Suppl. Fig. 3A-C) but subsequently normalized to control levels by 6 months of age (Suppl. Fig. 3J-L). There was no detectable alteration in Alz50 IR in AAV-APOE4-expressing mice at either ages (Suppl. Fig. 3 D-F, M-O). These data are supported by immunostaining with p62/sequestome-1 antibody, a generalized marker of autophagy dysfunction and inclusion pathology [22] which failed to show any APOE4-induced effects (Suppl. Fig. 3 G-I, P-R). We next investigated NFT-type insoluble tau burden using histological and biochemical methods (Fig. 4). Silver staining using the Gallyas method did not reveal altered NFT-type pathology in the Tg mice at 4 months (Fig. 4a–c) or at 6 months (Fig. 4l–n). Immunoblotting of sarkosyl insoluble cellular fraction using two ptau antibodies, CP13 and PHF1, also supported our immunohistochemistry data (Fig. 4d–g, o–r). Surprisingly, we observed a trend towards decreased endogenous mouse tau levels in APOE4-expressing 6-month-old Tg mice compared to control Tg mice (Fig. 4s, t, $p = 0.070$), though no such effect was observed at 4 months (Fig. 4h, i). We did not observe any changes in the levels of insoluble human total tau at either age in these mice (Fig. 4j, k, u, v).

Effect of APOE4 expression on synaptic protein profile and hippocampal cell counts in rTg4510 mice.

Since *APOE4* positive individuals may be at a higher risk for regional brain atrophy and functional decline [23, 24], we evaluated hippocampal CA neuron count and cortical thickness indicative of neuronal integrity. Normally, starting around 5 months of age, naïve Tg mice show profound tau-induced neuronal loss in the hippocampus as well as altered levels of synaptic proteins [25]. Our results indicate that APOE4 expression did not affect hippocampal CA1–3 neuronal counts, or cortical thickness, at 4 or 6 months of age (Fig. 5a–c and j–l, respectively) as compared to naïve control Tg mice. Further, using a panel of synaptic protein markers, we examined whether APOE4 induced any alterations at the level of synapses in these Tg mice. We did not observe appreciable changes in the levels of synaptogyrin 3, synaptophysin,

Fig. 3 Analysis of ptau epitopes in APOE4 expressing rTg4510 mice. ▶ Neonatal rTg4510 mice injected with AAV-APOE4 and aged to 4 months (**a–i**) or 6 months old (**j–r**). Representative images of CP13 immunoreactivity from 4-month-old mice are shown from different regions of the cortex and hippocampal CA1 (**a**). Scale bar: 100 μm. Quantitation of the immunostaining in 4-month-old mice is presented as % immunoreactivity in the cortex (Ctx) or hippocampus (Hpc) (**b, c**). $n = 7$ mice/group. Unpaired *t* test. Following western blotting with CP13, PHF1 and T49 antibodies (**d, f, h**) using S1 soluble brain extracts, bands were standardized to GAPDH, a housekeeping gene, and quantitated (**e, g, i**) for the 4-month group. $n = 6$ mice/group. Unpaired *t* test. Representative images of CP13 immunoreactivity from 6-month-old mice are shown (**j**), and the data quantitated as % immunoreactivity in the cortex (Ctx) or hippocampus (Hpc) (**k, l**). $n = 5$-10 mice/group. Scale bar: 100 μm. Unpaired *t* test. Western blotting for different tau epitopes (CP13 and PHF1 and T49) (**m, o, q**). Quantitation of normalized signal for the 6-month-old group is shown (**n, p, r**). $n = 4$ mice/group Unpaired *t* test. *$p < 0.05$. Black symbols, male mice; gray symbols, female mice.

spinophilin, PSD95, vGlut1 or GlutR1 in the 4-month or the 6-month cohort (Fig. 5d-i, m-r).

APOE4 expression does not trigger early tau accumulation in the PS19 model of tauopathy.

To complement our studies in the rTg4510 model, we used the same AAV approach to over-express APOE4 in the brains of the PS19 model of tau pathology [16]. The PS19 model expresses human P301S mutant tau and has a protracted phase of disease onset and progression. In the PS19 mice, ptau is observed around 3 months of age whereas NFTs and synaptic abnormalities appear by 6 months of age [16]. As before, we injected AAV-APOE4 into cerebral ventricles of neonatal PS19 mice and aged these mice to 3 months. At this age, these mice are expected to begin to show ptau accumulation but should have negligible NFT pathology. Our expectation was that if APOE4 triggered pretangle pathology, we would see increased sarkosyl-insoluble tau as well as conformationally altered tau in the APOE4-expressing cohort but not in the control cohort. We confirmed that AAV-APOE4 transduction resulted in APOE4 expression in the brains of these mice (Suppl. Fig. 4) but did not alter expression of human tau (Fig. 6a, b), CP13-immunopositive ptau (Fig. 6c–f), or expression of endogenous murine tau (Fig. 6g, h). We also conducted immunohistochemical analysis with MC1 that showed that there was no induction of pretangle pathology at this age in the APOE4-expressing PS19 cohort (Fig. 6i, j). Using serial fractionation methods and western analysis, we found negligible quantities of human total tau (Fig. 6k, l) and no mouse tau (Fig. 6m) in the sarkosyl-insoluble cellular fraction. Because only an insignificant level of insoluble total human tau was detected in this fraction, we did not further explore the presence of ptau. Synaptic pathology has been documented in PS19 mice, with loss of synaptophysin levels as early as 3 months of age [16]. To understand whether APOE4 expression worsens synaptic pathology, we examined several synaptic markers, such

4 month rTg4510

6 month rTg4510
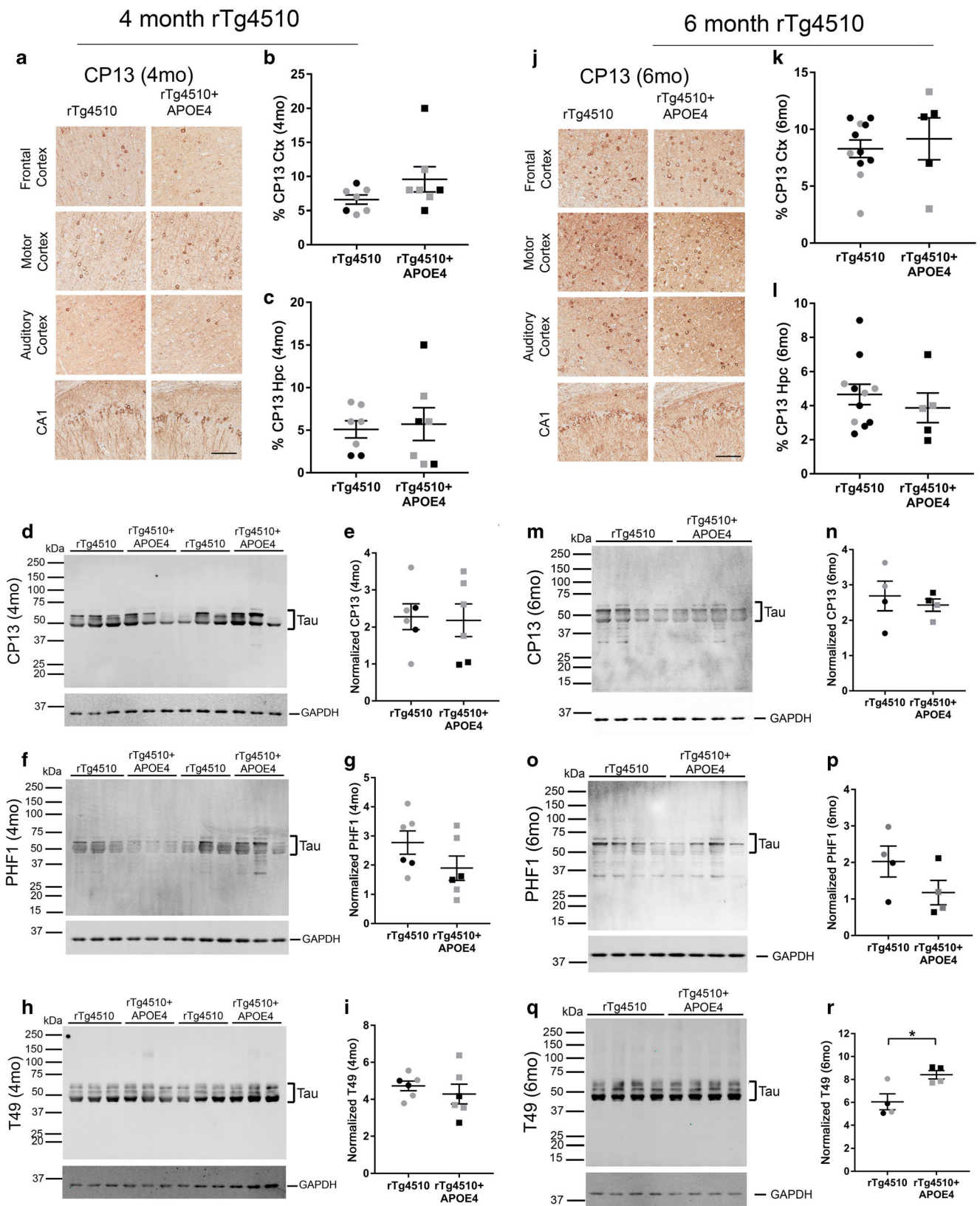
as synaptogyrin 3, synaptophysin, spinophilin, PSD95, vGlut1, and GluR1 in these PS19 mice (Fig. 7). Of the proteins examined, only vGlut1 was altered in APOE4-expressing PS19 mice

compared to age-matched PS19 controls, indicating altered glutamatergic neurotransmission in these mice (Fig. 7 e, $p < 0.01$).

Discussion

The relationship between the APOE4 isoform and tauopathy remains enigmatic. While human data suggest that Aβ links APOE4 and tau pathogenesis [11, 12], two recent seminal mouse studies have indicated that APOE can directly exert an isoform-dependent pathologic effect on tau pathogenesis and neurodegeneration [13, 14]. Here, using two models of human tau pathology rTg4510 and PS19, we have sought to test the hypothesis that neuronal/glial expression of AAV-human APOE4 can exacerbate or trigger tau pathology in the absence of Aβ. Our results indicate that (1) intracerebral expression of human APOE4 does not trigger formation of pretangles in PS19 model; (2) APOE4 does not exacerbate ptau pathology or NFT burden in the rTg4510 model; and (3) APOE4 expression does not have a major effect on synaptic protein levels in either mouse model of tauopathy. Together, these data suggest that neuronal-predominant expression of APOE4 does not necessarily synergize pathologically with tau and tau-related synaptic deficits in rodent models.

Understanding how APOE4 alters AD pathogenesis is critical for not only advancing a deeper mechanistic understanding of the pathogenic cascade in AD but also because APOE is druggable both directly [26, 27] or indirectly [28]. The role of APOE4 in exacerbating Aβ pathologies has been well-documented by various groups—it is widely accepted that the APOE4 isoform confers AD risk by reducing Aβ clearance, though there is some controversial data that APP/Aβ production can also be influenced by APOE isoforms [5–10]. Whether APOE also affects tau metabolism directly in an isoform-dependent manner leading to formation of AD-type NFT pathology has been a matter of intense debate. Though there is no direct link between NFT burden and APOE4 genotype in humans [29–32], some reports have shown increased association of APOE4 with tau pathology in AD patients with high amyloid burden [11, 12] as well as in a subset of PSP patients with additional AD pathologies [33]. Together, these results would suggest that APOE4 genotype does not necessarily predict tau pathology in primary and secondary tauopathies.

The mechanism underlying APOE isoform specific effects on tau remains undetermined. In patient brains, APOE is localized to neuritic plaques, vascular amyloid as well as NFTs [34]. Two early studies showed that human-derived APOE3, but not APOE4, binds to the microtubule-binding repeat region of recombinant non-phosphorylated tau in vitro [35, 36]. This suggested that APOE3-mediated binding and sequestering of tau may be physiologically protective by preventing tau from being available for post-translational modifications. However, one question remained as to whether these APOE proteins remained natively lipidated during these experimental conditions. A second study also identified mouse Apoe as a

Fig. 4 APOE4 expression does not induce formation of insoluble tau and ▶ tangle pathologies in rTg4510 mice. Neurofibrillary tangle pathology was analyzed using Gallyas silver staining method and insoluble tau was analyzed by western blotting of Sarkosyl-insoluble cellular fraction. Representative brain areas from Gallyas-stained 4-month-old rTg4510 mice are shown (**a**) and quantitated (**b**, **c**). Scale bar: 100 μm. *n* = 4–5 mice/group. Unpaired *t* test. Western blots of Sarkosyl-insoluble cell fraction from 4-month-old mice was probed for ptau (CP13 and PHF1), mouse tau (T49), and total human tau (CP27) (**d**–**k**). ptau bands were normalized to total human tau (**e**, **g**) while total mouse and human tau were presented as original values (**i**, **k**). *n* = 4–6/group. Unpaired *t* test. Corresponding results obtained from the 6-month-old rTg4510 mouse brains are shown—Gallyas staining (**l**–**n**) and western blotting of Sarkosyl-insoluble cell fraction probed for ptau (CP13 and PHF1), mouse tau (T49), and total human tau (CP27; **o**–**v**). *n* = 4–6/group. Scale bar, 100 μm. Unpaired *t* test. Black symbols, male mice; gray symbols, female mice.

binding partner for tau [37]. Interestingly, some reports also indicated that APOE fragments can be generated in an isoform-specific manner; C-terminal APOE4 fragments generated this way in neurons can bind to ptau and induce NFT type pathology [38, 39]. Though we have previously documented similar Apoe truncation products in an APP/Aβ model [40], we did not observe any APOE4 fragments in the AAV-APOE4/rTg4510 or AAV-APOE4/PS19 mice. Whether the absence of such neurotoxic APOE4 fragments was instrumental in blunting the potential toxic effects of APOE4 in our study remains under future investigation.

Two recent seminal papers have uncovered a pathogenic isoform-dependent role of APOE on tau metabolism. In the first study, bigenic PS19x*APOE* TR mice showed isoform-dependent pathologic effects on tau-mediated neurodegeneration with E4 > E3 > E2 [14]. A second study used AAV-mediated overexpression of human mutant tau in *APOE* TR mice and showed that APOE2 had a profound pathologic effect on tauopathy, which is consistent with its association with the human tauopathy, PSP [13]. In this second study, overexpression of AAV-tau in APOE4 mice led to significantly lower AT8-tau burden and Thioflavin S staining compared to APOE2 mice, such that the pathologic index of APOE isoform-tau interaction was E2 > E3~E4 [13]. These studies spurred our interest in a deeper investigation of APOE4 function in mouse models of human tauopathy.

Our results indicate that AAV-mediated expression of APOE4 in the brains of rTg4510 and PS19 mice has no appreciable effects on ptau, NFTs or synaptic protein expression. This is somehow inconsistent with the broad outcomes described in the Shi/Holtzman study [14] whereas our study is seemingly congruent with the Zhao/Bu study [13]. Our findings align with a prior study that observed no alteration in endogenous mouse tau phosphorylation by neuronal expression of human APOE4 [41], though we did observe subtle increases in total soluble mouse tau in the older rTg4510 cohort. However, since these studies used different

4 month rTg4510

6 month rTg4510
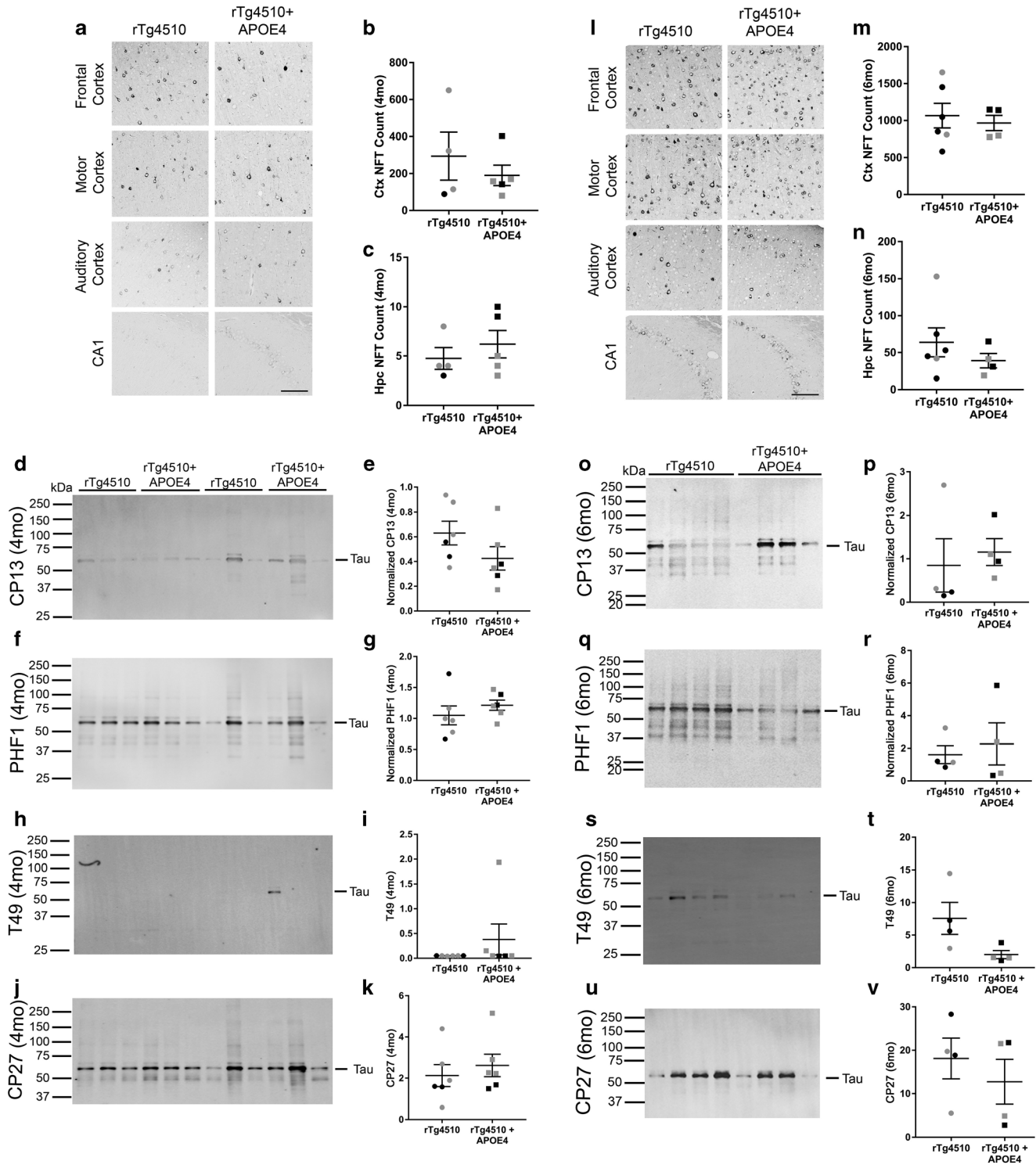
variations of mice and expression strategies, there could be multiple explanations regarding such seemingly disparate observations. The major difference between our study and the Shi/Holtzman study [14] is our usage of AAV-APOE4, which primarily resulted in neuronal expression of

APOE4, in adiition to some astrocytic expression. In APOE4 TR mice, we observed APOE immunoreactivity in astrocytes and blood vessels, but not in neurons. This pattern of expression is similar to what has been described for endogenous mouse Apoe [42]. Our study, which ectopically
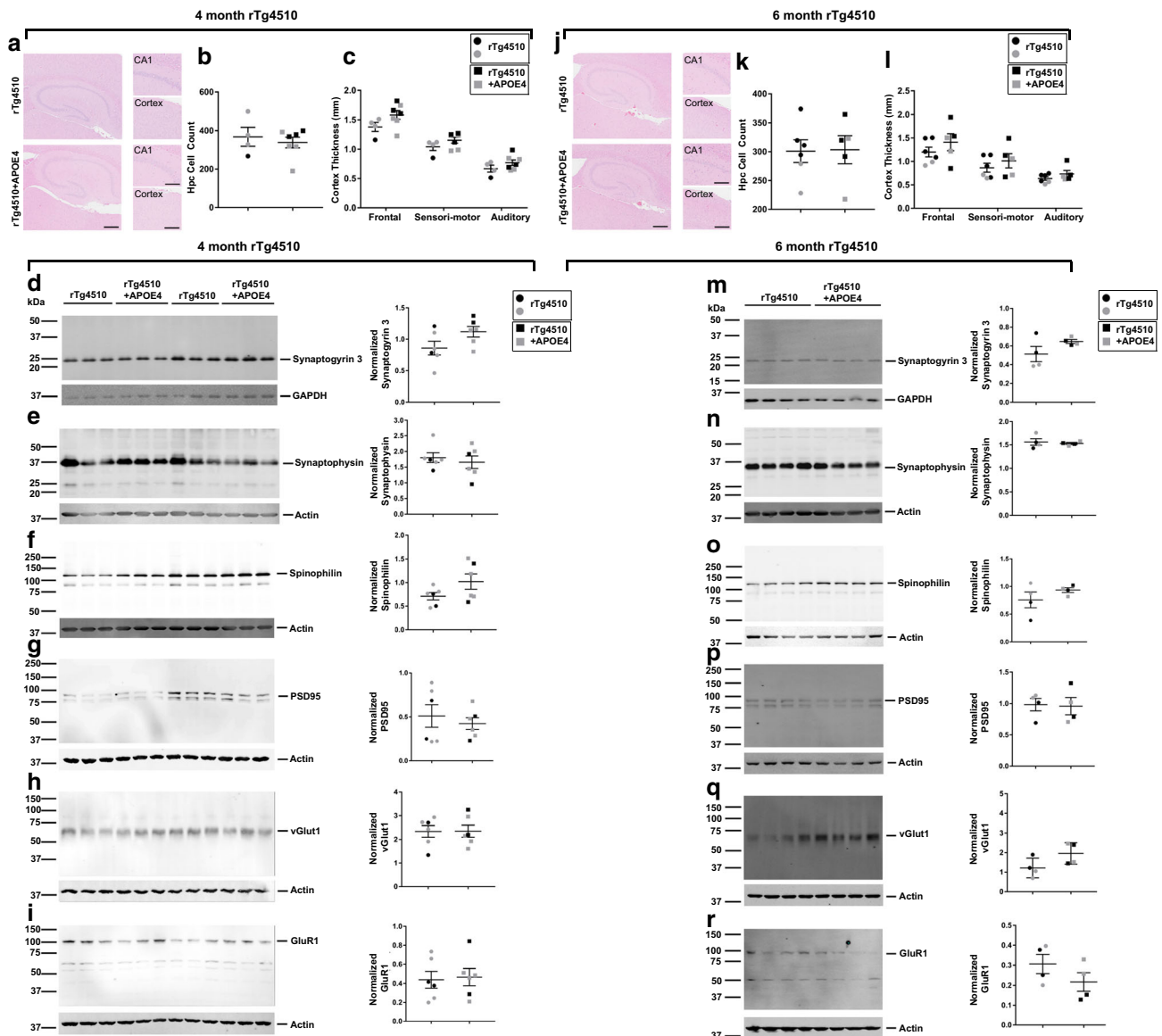
Fig. 5 Analysis of brain morphology and synaptic profiles in APOE4-expressing rTg4510 mice. Morphometric analysis of the forebrain was done by counting hippocampal CA1–3 neurons and by measuring cortical thickness (frontal cortex, motor/sensory cortex, and auditory cortex) in 4-month-old (**a**–**c**) or 6-month-old rTg4510 mice (**j**–**l**). This specific area was bounded by Bregma coordinates: 0.84 and 1.08 mm. Scale bar: 300 μm (larger panels on the left); 125 μm (smaller panels on the right). $n = 4$–6 mice/group.

Unpaired t test or two-way ANOVA. Synaptic protein profiles were analyzed by immunoblotting for synaptogyrin 3, synaptophysin, spinophilin, PSD95, vGlut1 and GluR1 in 4-month old (**d**–**i**) and in 6-month old rTg4510 mice (**m**–**r**). Indicated protein bands were quantified following normalization to either GAPDH or Actin as shown. $n = 6$/group (4-month rTg4510) and $n = 4$/group (6-month rTg4510). Unpaired t test. Black symbols, male mice; gray symbols, female mice

expressed human APOE4 in neurons did not produce an obvious increase in intra-neuronal ptau pathology in individual cells. Our study also primarily focused on determining whether APOE4 could accelerate the appearance of tau pathology by examining mice at relatively young ages (4 and 6 months for rTg4510 and 3 months for PS19). Notably, one of the previous studies analyzed tau pathology at older ages [14]. Another major difference between studies that use the APOE TR mice and our AAV model is the presence of mouse Apoe in our model. Both mouse Apoe and human APOE4 are highly amyloidogenic with some studies

suggesting that mouse Apoe may be markedly more amyloidogenic [43]; however, other studies have highlighted their functional differences in Aβ models [44] as well as atherosclerosis models [45]. Therefore, it is possible that presence of mouse Apoe modified the effects of human APOE4 in our study. Additionally, APOE TR mice have peripheral pools of human APOE4 which can possibly lead to vascular or blood/brain barrier alterations (reviewed in [46]). This is important as we and another report [42] show that transgene expression from the apoE locus results in high expression from blood vessel-associated cells. Whether the
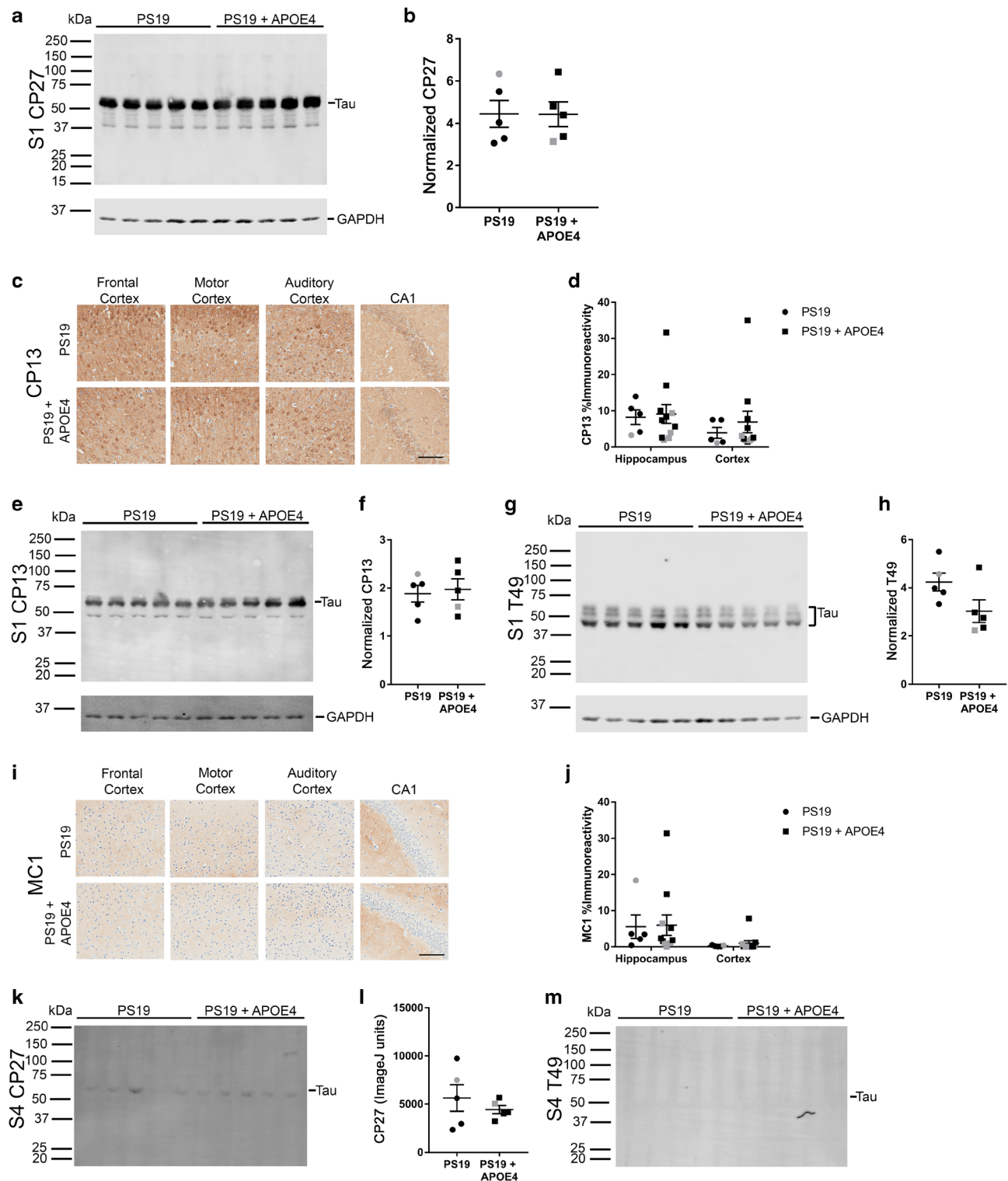
Fig. 6 APOE4 expression in PS19 mice and associated pathologies. Neonatal PS19 mice were injected with AAV-APOE4 or AAV-EGFP and aged to 3 months of age. APOE4 expression does not alter human tau transgene, as shown by CP27-immunoreactive total human tau (**a**). Quantification of tau protein band normalized to GAPDH loading control is shown (**b**). $n = 5$ mice/group. Unpaired t test. Representative images of CP13 immunoreactivity from 3-month-old mice are shown from different regions of the cortex and hippocampal CA1 (**c**). Scale bar: 100 μm. Quantitation of the immunostaining is presented as % immunoreactivity in the cortex and hippocampus (**d**). $n = 5–11$ mice/group. Two-way ANOVA.

Western blotting with PBS-extracted brain lysate (denoted as S1) was done using ptau antibody (CP13, **e, f**) and total mouse tau antibody (T49; **g, h**) with protein band normalized to GAPDH loading control (**f, h**). $n = 5$ mice/group. Unpaired t test. Pretangle tau levels were assessed by MC1 immunostaining in different areas of the cortex and hippocampus CA1 area (**i**) and data quantified as % immunoreactivity (**j**). Scale bar: 100 μm. $n = 5–11$ mice/group. Two-way ANOVA. Sarkosyl-insoluble cellular fraction (denoted as S4) was assessed for the presence of total human tau (**k, l**) and total mouse tau (**m**). $n = 5$ mice/group. Unpaired t test. Black symbols, male mice; gray symbols, female mice.

Fig. 7 Analysis of synaptic profile in APOE4-expressing PS19 mice. Synaptic protein profile was analyzed by immunoblotting for synaptogyrin 3, synaptophysin, spinophilin, PSD95, vGlut1, and GluR1 in 3 month old AAV-APOE4 or control PS19 mice (**a–f**). Indicated protein bands were quantified following normalization to Actin as shown. $n = 5$ mice/group. Unpaired t test, **$p < 0.01$. Black symbols, male mice; gray symbols, female mice
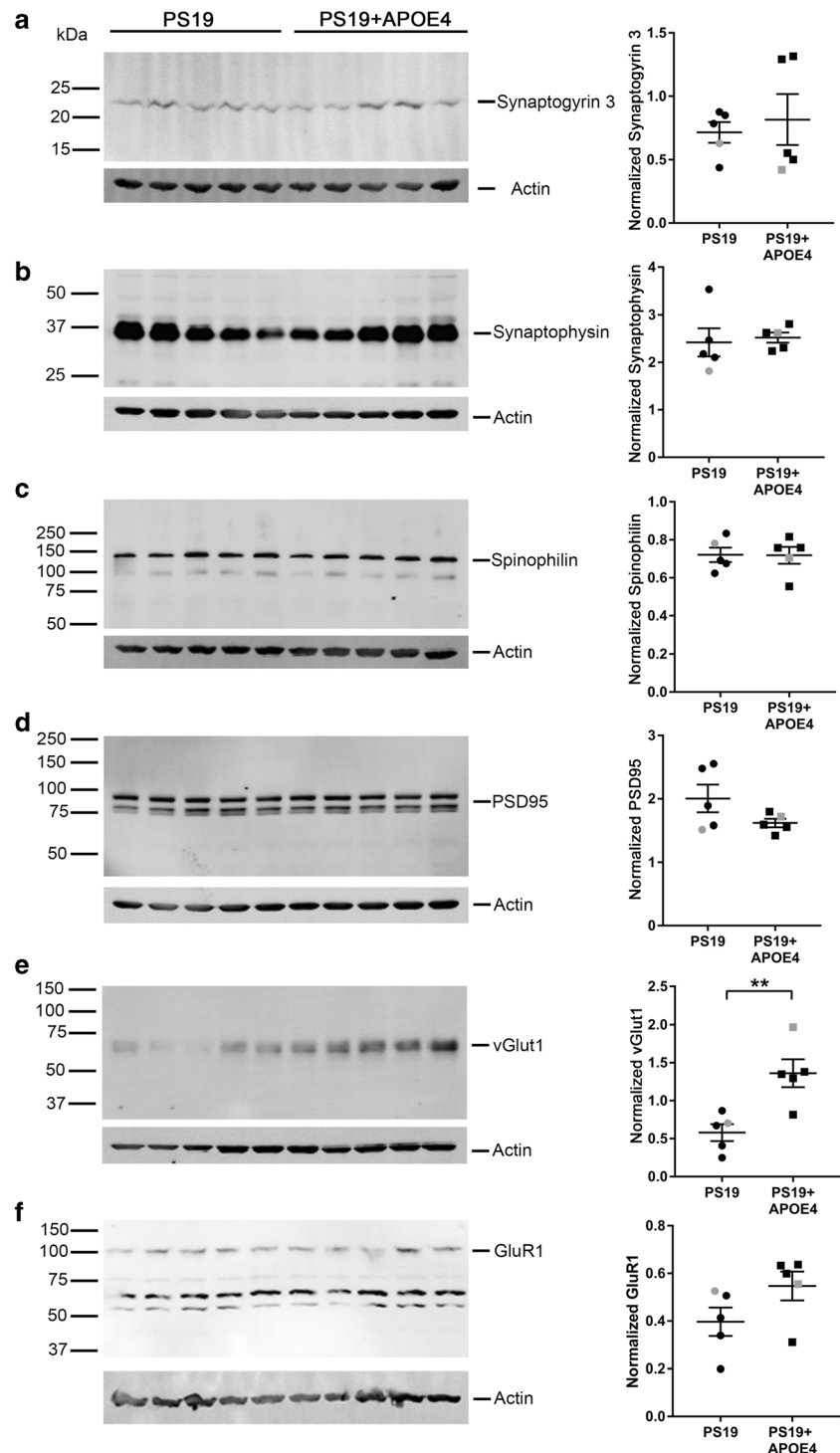
peripheral pool of APOE4 in APOE TR mice used in the previous studies [13, 14] but absent in our current AAV-APOE4 model can explain some of the disparate observations in E4-related neurodegeneration, and tauopathy remains a focus for future studies. Additionally, there can be some unique challenges in the AAV-mediated transduction system compared to traditional transgenic mice. For example, there can be inter-sample variability based on

transduction patterns as well as gradual loss of transgene expression as mice get older in AAV cohorts, features that are not generally observed in germline stable transgenic models.

In summary, we demonstrate that primarily neuronal targeted expression of human APOE4 does not trigger accelerated tauopathy in two widely used mouse models of tau pathology. Our findings suggest that any effect

APOE4 may have in modulating tau pathology is unlikely to involve a direct triggering interaction between APOE and tau and probably could be a result of non-cell autonomous signaling pathways.

Authors' Contributions PC conceived the study, designed all figures and wrote the manuscript. EJK performed the experiments with help of EGDLC, MW, TW, and PC. JL provided rTg4510 breeders, and PMS provided APOE4 TR mice. PEC cloned APOE4, and DR packaged the AAV. TEG and DRB provided scientific input. EJK, EGDLC, TW, DRB and PC performed data analysis. All authors reviewed the manuscript and approved its final version.

Availability of Data and Materials All the data supporting the conclusions of this article are included within the article and its supplementary information files.

Compliance with ethical standards

Conflict of Interest The authors declare that they have no conflict of interest.

Ethics Approval All animal experiments were approved by the University of Florida IACUC.

Consent for Publication This manuscript has been approved for publication by all authors.

References

1. Corder EH, Saunders AM, Strittmatter WJ, Schmechel DE, Gaskell PC, Small GW, Roses AD, Haines JL et al (1993) Gene dose of apolipoprotein E type 4 allele and the risk of Alzheimer's disease in late onset families. Science 261:921–923
2. Leduc V, Jasmin-Bélanger S, Poirier J. (2010) APOE and cholesterol homeostasis in Alzheimer's disease. Trends Mol Med 16:469–477
3. Huang Y, Mahley RW (2014) Apolipoprotein E: structure and function in lipid metabolism, neurobiology, and Alzheimer's diseases. Neurobiol Dis 72:3–12
4. Liu CC, Kanekiyo T, Xu H, Bu G (2013) Apolipoprotein E and Alzheimer disease: risk, mechanisms and therapy. Nat Rev Neurol 9:106–118
5. Reiman EM, Chen K, Liu X, Bandy D, Yu M, Lee W, Ayutyanont N, Keppler J et al (2009) Fibrillar amyloid-beta burden in cognitively normal people at 3 levels of genetic risk for Alzheimer's disease. Proc Natl Acad Sci U S A 106:6820–6825
6. Huang YA, Zhou B, Wernig M, Sudhof TC (2017) ApoE2, ApoE3, and ApoE4 differentially stimulate APP transcription and Abeta secretion. Cell 168:427–441
7. Castellano JM, Kim J, Stewart FR, Jiang H, DeMattos RB, Patterson BW, Fagan AM, Morris JC et al (2011) Human apoE isoforms differentially regulate brain amyloid-beta peptide clearance. Sci Transl Med 3(89):89ra57
8. Bales KR, Liu F, Wu S, Lin S, Koger D, DeLong C, Hansen JC, Sullivan PM et al (2009) Human APOE isoform-dependent effects on brain beta-amyloid levels in PDAPP transgenic mice. J Neurosci 29:6771–6779
9. DeMattos RB, Cirrito JR, Parsadanian M, May PC, O'Dell MA, Taylor JW, Harmony JA, Aronow BJ et al (2004) ApoE and clusterin cooperatively suppress Abeta levels and deposition: evidence that ApoE regulates extracellular Abeta metabolism in vivo. Neuron 41:193–202
10. Koistinaho M, Lin S, Wu X, Esterman M, Koger D, Hanson J, Higgs R, Liu F et al (2004) Apolipoprotein E promotes astrocyte colocalization and degradation of deposited amyloid-beta peptides. Nat Med 10:719–726
11. Farfel JM, Yu L, De Jager PL, Schneider JA, Bennett DA (2016) Association of APOE with tau-tangle pathology with and without beta-amyloid. Neurobiol Aging 37:19–25
12. Hohman TJ, Dumitrescu L, Barnes LL, Thambisetty M, Beecham G, Kunkle B, Gifford KA, Bush WS et al (2018) Sex-specific association of apolipoprotein E with cerebrospinal fluid levels of tau. JAMA Neurol 75:989–998
13. Zhao N, Liu CC, Van Ingelgom AJ, Linares C, Kurti A, Knight JA, Heckman MG, Diehl NN et al (2018) APOE epsilon2 is associated with increased tau pathology in primary tauopathy. Nat Commun 9:4388
14. Shi Y, Yamada K, Liddelow SA, Smith ST, Zhao L, Luo W, Tsai RM, Spina S et al (2017) ApoE4 markedly exacerbates tau-mediated neurodegeneration in a mouse model of tauopathy. Nature 549:523–527
15. Santacruz K, Lewis J, Spires T, Paulson J, Kotilinek L, Ingelsson M, Guimaraes A, DeTure M et al (2005) Tau suppression in a neurodegenerative mouse model improves memory function. Science 309:476–481
16. Yoshiyama Y, Higuchi M, Zhang B, Huang SM, Iwata N, Saido TC, Maeda J, Suhara T et al (2007) Synapse loss and microglial activation precede tangles in a P301S tauopathy mouse model. Neuron 53:337–351
17. Knouff C, Hinsdale ME, Mezdour H, Altenburg MK, Watanabe M, Quarfordt SH, Sullivan PM, Maeda N (1999) Apo E structure determines VLDL clearance and atherosclerosis risk in mice. J Clin Invest 103:1579–1586
18. Chakrabarty P, Rosario A, Cruz P, Siemienski Z, Ceballos-Diaz C, Crosby K, Jansen K, Borchelt DR et al (2013) Capsid serotype and timing of injection determines AAV transduction in the neonatal mice brain. PLoS One 8:e67680
19. Koller EJ, Gonzalez De La Cruz E, Machula T, Ibanez KR, Lin W-L, Williams T, Riffe CJ, Ryu D et al (2019) Combining P301L and S320F tau variants produces a novel accelerated model of tauopathy. Hum Mol Genet 28:3255–3269. https://doi.org/10.1093/hmg/ddz151
20. Kuninaka N, Kawaguchi M, Ogawa M, Sato A, Arima K, Murayama S, Saito Y (2015) Simplification of the modified Gallyas method. Neuropathology 35:10–35
21. Ramsden M, Kotilinek L, Forster C, Paulson J, McGowan E, SantaCruz K, Guimaraes A, Yue M et al (2005) Age-dependent neurofibrillary tangle formation, neuron loss, and memory impairment in a mouse model of human tauopathy (P301L). J Neurosci 25(46):10637–10647
22. Piras A, Collin L, Gruninger F, Graff C, Ronnback A (2016) Autophagic and lysosomal defects in human tauopathies: analysis of post-mortem brain from patients with familial Alzheimer disease, corticobasal degeneration and progressive supranuclear palsy. Acta Neuropathol Commun 4:22
23. Agosta F, Vossel KA, Miller BL, Migliaccio R, Bonasera SJ, Filippi M, Boxer AL, Karydas A et al (2009) Apolipoprotein E epsilon4 is associated with disease-specific effects on brain atrophy in Alzheimer's disease and frontotemporal dementia. Proc Natl Acad Sci U S A 106:018–022
24. Wisdom NM, Callahan JL, Hawkins KA (2011) The effects of apolipoprotein E on non-impaired cognitive functioning: a meta-analysis. Neurobiol Aging 32:63–74

25. Kopeikina KJ, Polydoro M, Tai HC, Yaeger E, Carlson GA, Pitstick R, Hyman BT, Spires-Jones TL (2013) Synaptic alterations in the rTg4510 mouse model of tauopathy. J Comp Neurol 521:1334–1353

26. Liao F, Li A, Xiong M, Bien-Ly N, Jiang H, Zhang Y, Finn MB, Hoyle R et al (2018) Targeting of nonlipidated, aggregated apoE with antibodies inhibits amyloid accumulation. J Clin Invest 128:2144–2155

27. Kim J, Eltorai AE, Jiang H, Liao F, Verghese PB, Kim J, Stewart FR, Basak JM et al (2012) Anti-apoE immunotherapy inhibits amyloid accumulation in a transgenic mouse model of Abeta amyloidosis. J Exp Med 209:2149–2156

28. Geifman N, Brinton RD, Kennedy RE, Schneider LS, Butte AJ (2017) Evidence for benefit of statins to modify cognitive decline and risk in Alzheimer's disease. Alz Res Ther 9:10

29. Morris JC, Roe CM, Xiong C, Fagan AM, Goate AM, Holtzman DM, Mintun MA (2010) APOE predicts amyloid-beta but not tau Alzheimer pathology in cognitively normal aging. Ann Neurol 67:122–131

30. Vemuri P, Wiste HJ, Weigand SD, Knopman DS, Shaw LM, Trojanowski JQ, Aisen PS, Weiner M et al (2010) Effect of apolipoprotein E on biomarkers of amyloid load and neuronal pathology in Alzheimer disease. Ann Neurol 67:308–316

31. Caselli RJ, Walker D, Sue L, Sabbagh M, Beach T (2010) Amyloid load in nondemented brains correlates with APOE e4. Neurosci Lett 473:168–171

32. Mattsson N, Ossenkoppele R, Smith R, Strandberg O, Ohlsson T, Jogi J, Palmqvist S, Stomrud E et al (2018) Greater tau load and reduced cortical thickness in APOE epsilon4-negative Alzheimer's disease: a cohort study. Alz Res Ther 10:77

33. Tsuboi Y, Josephs KA, Cookson N, Dickson DW (2003) APOE E4 is a determinant for Alzheimer type pathology in progressive supranuclear palsy. Neurology 6:240–245

34. Namba Y, Tomonaga M, Kawasaki H, Otomo E, Ikeda K (1991) Apolipoprotein E immunoreactivity in cerebral amyloid deposits and neurofibrillary tangles in Alzheimer's disease and kuru plaque amyloid in Creutzfeldt-Jakob disease. Brain Res 541:163–166

35. Strittmatter WJ, Saunders AM, Goedert M, Weisgraber KH, Dong LM, Jakes R, Huang DY, Pericak-Vance M et al (1994) Isoform-specific interactions of apolipoprotein E with microtubule-associated protein tau: implications for Alzheimer disease. Proc Natl Acad Sci U S A 91(23):11183–11186

36. Fleming LM, Weisgraber KH, Strittmatter WJ, Troncoso JC, Johnson GV (1996) Differential binding of apolipoprotein E isoforms to tau and other cytoskeletal proteins. Exp Neurol 138(2):252–260

37. Liu C, Song X, Nisbet R, Gotz J (2016) Co-immunoprecipitation with tau isoform-specific antibodies reveals distinct protein interactions and highlights a putative role for 2N tau in disease. J Biol Chem 291:8173–8188

38. Huang Y, Liu XQ, Wyss-Coray T, Brecht WJ, Sanan DA, Mahley RW (2001) Apolipoprotein E fragments present in Alzheimer's disease brains induce neurofibrillary tangle-like intracellular inclusions in neurons. Proc Natl Acad Sci U S A 98:8838–8843

39. Brecht WJ, Harris FM, Chang S, Tesseur I, Yu GQ, Xu Q, Dee FJ, Wyss-Coray T et al (2004) Neuron-specific apolipoprotein e4 proteolysis is associated with increased tau phosphorylation in brains of transgenic mice. J Neurosci 24:2527–2534

40. Chakrabarty P, Li A, Ceballos-Diaz C, Eddy JA, Funk CC, Moore B, DiNunno N, Rosario AM et al (2015) IL-10 alters immunoproteostasis in APP mice, increasing plaque burden and worsening cognitive behavior. Neuron 85:519–533

41. Lesuisse C, Xu G, Anderson J, Wong M, Jankowsky J, Holtz G, Gonzalez V, Wong PC et al (2001) Hyper-expression of human apolipoprotein E4 in astroglia and neurons does not enhance amyloid deposition in transgenic mice. Hum Mol Genet 10:2525–2537

42. Xu Q, Bernardo A, Walker D, Kanegawa T, Mahley RW, Huang Y (2006) Profile and regulation of apolipoprotein E (ApoE) expression in the CNS in mice with targeting of green fluorescent protein gene to the ApoE locus. J Neurosci 26:4985–4994

43. Fagan AM, Watson M, Parsadanian M, Bales KR, Paul SM, Holtzman DM (2002) Human and murine ApoE markedly alters A beta metabolism before and after plaque formation in a mouse model of Alzheimer's disease. Neurobiol Dis 9:305–318

44. Liao F, Zhang TJ, Jiang H, Lefton KB, Robinson GO, Vassar R, Sullivan PM, Holtzman DM (2015) Murine versus human apolipoprotein E4: differential facilitation of and co-localization in cerebral amyloid angiopathy and amyloid plaques in APP transgenic mouse models. Acta Neuropathol Commun 3:70

45. Eberle D, Kim RY, Luk FS, de Mochel NS, Gaudreault N, Olivas VR, Kumar N, Posada JM et al (2012) Apolipoprotein E4 domain interaction accelerates diet-induced atherosclerosis in hypomorphic Arg-61 apoe mice. Arterioscler Thromb Vasc Biol 32:1116–1123

46. Tai LM, Thomas R, Marottoli FM, Koster KP, Kanekiyo T, Morris AW, Bu G (2016) The role of APOE in cerebrovascular dysfunction. Acta Neuropathol 131:709–723